Wave-current interaction in tidal fronts

Burkard Baschek

Woods Hole Oceanographic Institution, MA, USA

Abstract. Tidal fronts are a common feature of the coastal ocean. They are formed by the interaction of tidal currents with topography and are characterized by surface convergence zones with strong gradients in density and current speed. Waves – or even small disturbances formed at low wind speed – that travel into these areas are slowed down by the currents and tend to steepen and break. Because the location of wave breaking is therefore highly predictable, tidal fronts form an ideal and easily accessible natural laboratory for studying wave-current and wave-wave interactions. The conditions in the fronts favor the formation of statistically extreme waves, i.e. waves with heights of up to twice the significant wave height. Due to the small spatial scales of tidal fronts, it is possible to observe the history of these waves in space and time simultaneously. In spite of the different scales of the waves, the principal physics of the formation mechanisms may be applicable to the open ocean case where rogue waves represent a significant threat to ship traffic and offshore structures.

Introduction

Tidal fronts can be found in the coastal ocean where strong tidal currents interact with topography. At the sea surface, convergence zones with strong gradients in density and current speed are formed. Tidal fronts are areas of intense mixing but are also interesting for air-sea gas exchange (*Baschek*, 2003) and underwater acoustics due to large amounts of entrained gas bubbles. They also deserve attention due to a strong biological response to the physical processes in the fronts, like krill and fish aggregations (*Simard et al.*, 2002).

But tidal fronts are also interesting because of their pronounced effect on surface waves and are therefore natural laboratories for studying wave-current interaction. Surface gravity waves, that were generated by wind or any other disturbances of the sea surface, travel into the convergence zone, steepen due to the effect of the currents, and tend to break. This situation is similar to wave breaking in shallow water.

Areas of strong currents are known to be potentially hazardous for ship traffic as waves can be getting short and steep (*D. Masson*, 1996). Tidal currents can change sea state conditions within minutes as the direction of the tidal current changes.

In addition, it has been shown that strong oceanic currents favor the formation of rogue waves (*Wu and Yao*, 2004). These waves are characterized by their extreme statistics with wave heights of 1.5-2.0 times the significant wave height of the surrounding wave field. With wave heights of up to 35 m, these waves are a potential threat for ships and offshore structures.

While rogue waves have long been treated as ”sailor's myth”, it has now been recognized that they are a rare but frequent oceanic feature. In January 1995, for example, a rogue wave of 25.6 m was measured from the Norwegian oil drilling platform Draupner in the North Sea (*Clauss*, 2002). In February 2001, the German cruise ship Bremen was hit in the Southern Ocean by a wave of estimated 30-35 m height and only 2 weeks later the Caledonian Star encountered a wave of similar height in the same area. In April 2005, the cruise ship Norwegian Dawn was severly damaged by a rogue wave of more than 20 m off Florida. Also a recent investigation of satellite images suggests that rogue waves occur quite frequently (*MaxWave*). During a period of three weeks in 1996, several rogue waves could be observed in the Southern Ocean.

Observations of rogue waves are extremely difficult to obtain as these waves are relatively rare and occur under rough conditions. So far, only a few rogue waves have been measured with wave gauges (e.g. *Clauss* (2002)) or recently also from satellite (*MaxWave*). For a better understanding of the formation process and for developing a forecasting system for ship traffic it is, however, necessary to obtain more measurements of these waves, in particular observations of the formation process of these waves as well as their subsequent evolution and decay.

Simultaneous measurements of statistically extreme waves in time and space can be easily carried out in the coastal environment. Although the waves there are much smaller than oceanic rogue waves, observations in tidal fronts may provide valuable insight into the formation process of these waves which may be applicable to the open ocean case.

In this paper, the behavior of waves traveling on a spatially varying current is described. First, a model of wave-current interaction is reviewed, which then leads to considerations on wave breaking and energy dissipation. Some of these considerations may be applicable to the formation process of rogue waves in areas of strong oceanic currents.

Tidal fronts

Tidal fronts are generated by the interaction of strong tidal currents with topography and are a common feature of the coastal ocean. They can be defined as sharp transition zones between two water masses of different density and (tidal) current speed. At the sea surface, a pronounced front line of 1-20 m width can be observed (Figure 1). Due to the strong shear across the front, energetic eddies are formed that enhance the mixing between the two water masses on both sides of the front. This front extends into the water column to depths of typically 50-150 m and forms an interface that may be tilted due to density differences between the two water masses (*Farmer et al.*, 2002; *Baschek*, 2003).

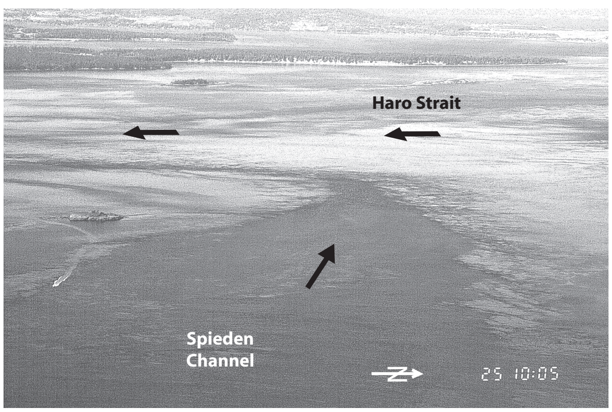

Figure 1. Aerial view of a tidal front in the Fraser Estuary, British Columbia. The arrows indicate the main flow direction.

Tidal Fronts can be formed by three different mechanisms (Figure 2):

- Type I: Inflow of dense water from an adjacent channel and plunging flow into intermediate depths;
- Type II: Flow separation processes past a headland, i.e. flow-topography interaction at a vertical boundary (*Farmer et al.*, 2002);
- Type III: Flow over a shallow sill, i.e. flow-topography interaction at a horizontal boundary.

All of these tidal fronts are characterized by converging flow at the sea surface with either both water masses flowing towards the front or one of them being stagnant.

Waves traveling into these fronts tend to steepen and break due to the effect of the changing currents (Figure 3).

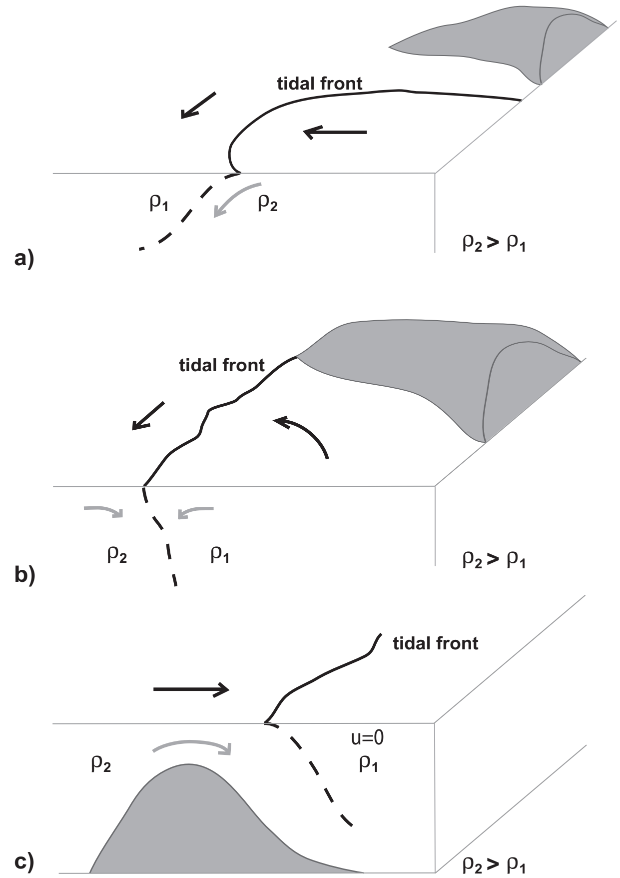

Figure 2. Different types of tidal fronts. a) Inflow of dense water from an adjacent channel; b) flow separation past a headland; c) flow over a shallow sill. For explanations see text.

For a wave, it is equivalent if it is riding on a current towards the front or if it is approaching the front from still water: in a reference frame moving with the water, the wave always encounters an opposing current. The difference between the two cases only has to be considered if the location of wave breaking relative to the tidal front is of importance. The general problem, however, is adequately described by the first case. For simplicity, we will therefore limit our considerations to the case where a wave travels from still water to an opposing current.

The observations presented in this paper were made in the Haro Strait region of the Fraser Estuary, BC, Canada (Figure 4). Special attention was given to the tidal fronts at Stuart Island, Battleship Island, and Boundary Pass.

Wave-current interaction

In the following, we will describe the behavior of a wave that encounters an opposing current with a model of wave action conservation (*Bretherton and Garrett*, 1969). We assume that the processes can be described by linear wave the-

Figure 3. Wave breaking in the convergence zone of a tidal front in the Fraser Estuary.

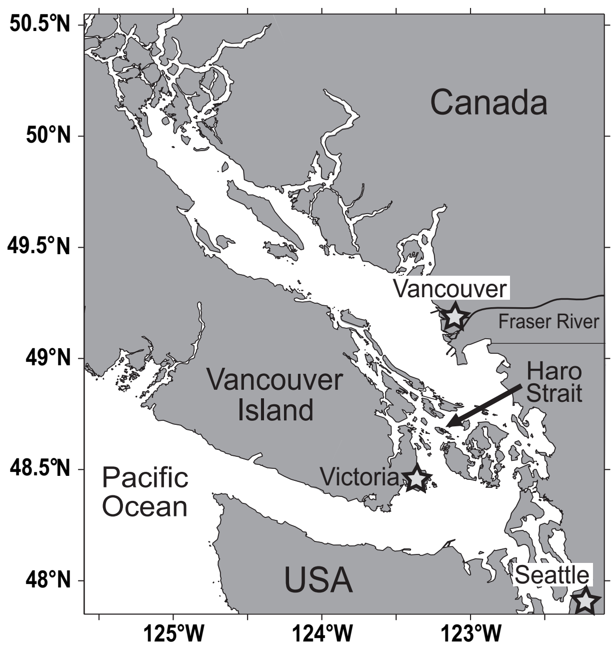

Figure 4. The Fraser Estuary in British Columbia, Canada.

ory and that wave-wave interactions can be neglected.

In the following, variables in a reference frame moving with the currents have no subscript while variables in a medium at rest ($u = 0$; u is the horizontal current speed) are marked by the subscript '0'.

Since the water depth in the tidal fronts is $H > 60\,\mathrm{m}$ and is therefore larger than the wave length $\lambda \ll 2H$, the waves can be treated as deep water waves (short waves) with a phase speed $c = \sqrt{g/k}$, where g is the gravitational acceleration and k the wave number. The wave energy is transported with the group velocity $c_g = c/2$.

For waves traveling on a current, the frequency for a fixed reference frame is

$$ku + \omega = const. \equiv \omega_0 \quad , \tag{1}$$

where ω_0 is the frequency at $u = 0$ (*Phillips*, 1977). With the expressions $\omega = \sqrt{gk}$ and $c = \sqrt{g/k}$ we get

$$k(u + c) = k_0 c_0 \quad , \tag{2}$$

from which we can derive a quadratic equation for the phase speed c with the solution

$$\frac{c}{c_0} = \frac{1}{2} + \frac{1}{2}\sqrt{1 + \frac{4u}{c_0}} \quad . \tag{3}$$

Bretherton and Garrett (1969) derived a conservation equation for wave action, that is valid for waves traveling on a slowly varying current (i.e. the currents change only little over a wave length)

$$\frac{\partial}{\partial t}\left(\frac{E}{\omega}\right) + \nabla \cdot \left\{(\mathbf{u} + \mathbf{c}_g)\frac{E}{\omega}\right\} = 0 \quad , \tag{4}$$

where $\mathbf{u}$ and $\mathbf{c}_g$ are the vectors of the current speed and group velocity. For steady wave trains traveling in x-direction this can be further simplified

$$\frac{d}{dx}\left\{(u + c_g)\frac{E}{\omega}\right\} = 0 \quad , \tag{5}$$

so that we get for deep water waves, using $\omega = g/c$ and the equations for phase and group speed

$$E\left(u + \frac{1}{2}c\right)c = const. \equiv \frac{1}{2}E_0 c_0^2 \quad . \tag{6}$$

Together with the wave energy equation $E = \rho g a^2/2$ we finally get an expression for the wave amplitude a (*Phillips*, 1977)

$$\frac{a}{a_0} = \frac{c_0}{\sqrt{(2u + c)c}} \quad . \tag{7}$$

The wave energy is then given by $E/E_0 = (a/a_0)^2$ and is shown by the gray curve in Figure 5 as a function of the normalized current speed u/c_0. The waves travel from left to right (for explanations of the other curves see below). At $u = 0$, $E/E_0 = 1$ by definition and E/E_0 goes towards infinity as u goes towards the negative group speed of the wave ($u/c_0 = -1/4$).

Breaking waves on a current

In reality, waves do not reach infinite amplitudes but break when they reach a certain critical steepness ka, given by the product of wave number k and amplitude a. This value is given by *Longuet-Higgins* (1969) as $ka = 1/2$. Other authors use a limiting steepness of $ka = 0.31$ (*Duncan*, 1980) or found values ranging from $ka = 0.15$ to $ka = 0.36$ if currents are present (*Wu and Yao*, 2004). For our considerations the exact value is not critical and we will therefore use for simplicity $ka = 1/2$.

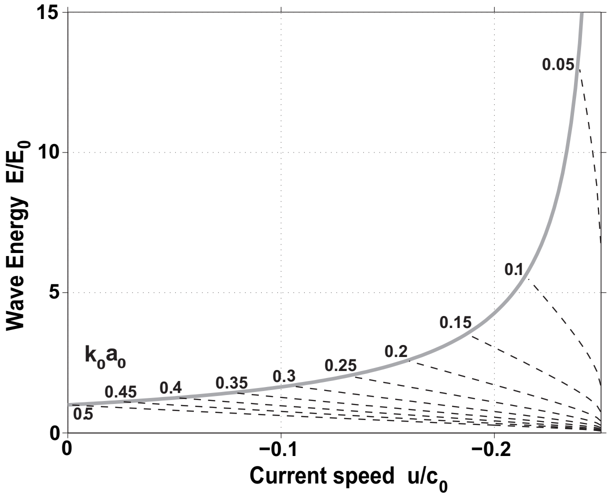

Figure 5. Wave energy as a function of current speed. Current speed and amplitude are scaled with the values for a medium at rest ($u = 0$). The wave energy in the absence of wave breaking (solid gray curve) is plotted together with the wave energy for a breaking wave (dashed black curves, equation 8) of initial steepness k_0a_0 (black numbers).

Obviously, the location at which the wave breaks, the amplitude of the wave, and also the distribution of dissipated energy depends on the current speed but also on the initial wave number k_0 and wave amplitude a_0. $E/E_0 = (a/a_0)^2$ describes the wave energy for a given current speed and is plotted in Figure 5. At some point the wave reaches its critical steepness and breaks. To derive the equation for the energy of a breaking wave, the break condition $ka = 1/2$ is multiplied by $1/(ka_0)$. Together with the expression $(c/c_0)^2 = k_0/k$ we get

$$\frac{a}{a_0} = \left(\frac{c}{c_0}\right)^2 \frac{1}{2k_0a_0} \quad , \tag{8}$$

where c/c_0 is given by equation (3). For waves with high initial steepness k_0a_0 this will happen at low current speeds and for waves with lower initial steepness at higher current speeds. The amplitude at which the wave exceeds the break criterium decreases as the wave travels further against the current, because the wave number increases with current speed. The more the currents increase the more energy is lost by breaking. It should be noted though that due to the effect of the currents the difference of wave energy between two points of the curve is not equivalent to the energy lost by wave breaking (see below).

Amplitude and energy of a breaking wave

When the current speed equals or exceeds the negative group velocity $u/c_0 \geq -1/4$ (equation 3), the waves cannot proceed against the currents and will have to break somewhere in the convergence zone. To calculate the amplitude of a wave when it breaks, we insert equation (2) into equation (7), use $(c/c_0)^2 = k_0/k$, and multiply by $(a_0/a)^{3/2}$ yielding

$$\left(\frac{a_0}{a}\right)^{7/2} + \frac{k_0a_0}{ka}\left(\frac{a_0}{a}\right)^{1/2} - 2\left(\frac{k_0a_0}{ka}\right)^{3/2} = 0 \quad . \tag{9}$$

Together with the condition for wave breaking $ka = 1/2$ we get

$$\left(\frac{a_0}{a}\right)^{7/2} + 2k_0a_0\left(\frac{a_0}{a}\right)^{1/2} - 2(2k_0a_0)^{3/2} = 0 \quad . \tag{10}$$

This equation can be solved for the relative amplitude a/a_0 that is plotted in Figure 6 as the gray curve. It shows the situation for a wave traveling from still water (right) to fast opposing current (left). The corresponding current speed is indicated by the black dots and numbers. The amplitude at which the wave breaks depends only on its initial steepness and increases with decreasing k_0a_0. It goes towards infinity as k_0a_0 goes towards zero.

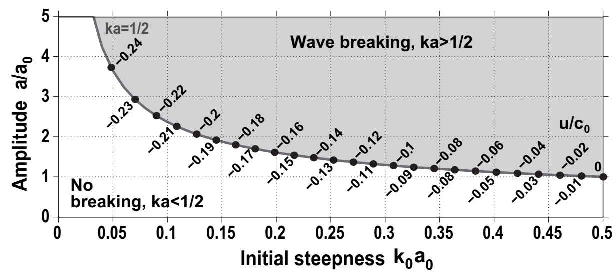

Figure 6. Relative change of the amplitude a/a_0 of a breaking wave as function of the initial wave steepness. The numbers indicate the corresponding current speed u/c_0 at which the wave starts to break.

The amplitude can be also normalized as k_0a and is plotted in Figure 7 as a function of current speed after multiplying equation (7) by k_0a_0. A wave of initial steepness k_0a_0 travels from left to right into the convergence zone until it breaks (gray curves). From then on it follows the black curve (in the absence of breaking it would follow the dashed gray curves), that is derived by multiplying equation (8) by k_0a_0.

Continuous and intermittent breaking

There are different types of breaking waves (*Galvin*, 1968) depending on environmental conditions like wind, currents, or bathymetry:

- Spilling breakers occur when the wave slowly reaches its critical steepness. The wave becomes unstable at the top and the “excess height” is lost by breaking in form of a whitecap (Figure 8a), which then flows down the front face of the wave.

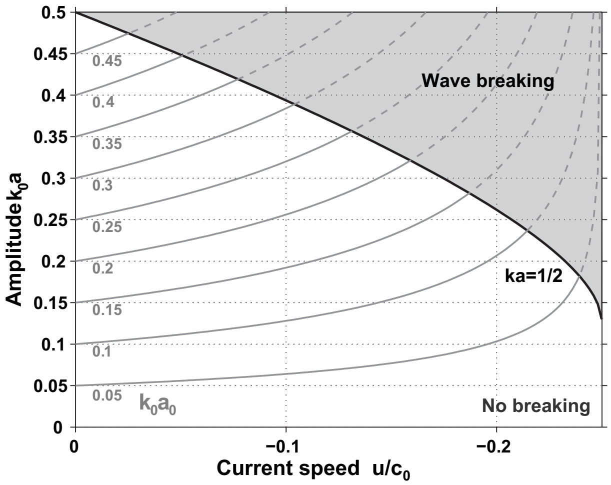

Figure 7. The gray curves show the normalized amplitude of a wave of initial steepness k_0a_0 (gray numbers) as a function of current speed u/c_0. After the wave reaches the critical value $ka = 1/2$ the amplitude is given by the black curve, or in the absence of breaking by the dashed gray curves.

- Plunging breakers occur when the wave breaks quickly. The crest curls over the front face, plunges forward, and falls into the base of the wave enclosing some larger amount of air while breaking (Figure 8b). Most of the wave energy is dissipated by one short break event.
- Collapsing and surging breakers occur when the wave crest remains unbroken and the wave base advances up a steep beach.

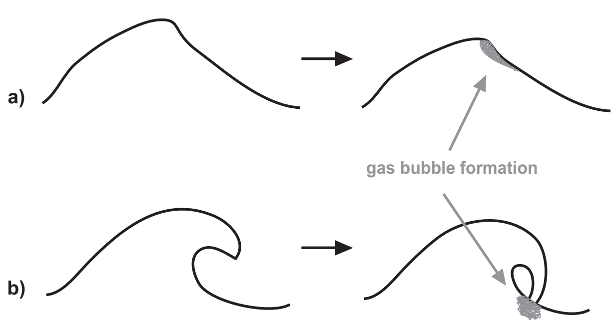

Figure 8. Sketch of a) spilling breaker and b) plunging breaker.

Observations show that spilling breakers are predominent in tidal fronts (Figure 3). We will therefore limit the following considerations to these waves. It is quite possible though that some waves break in a convergence zone as plunging breakers or some intermediate type of breaker. This is suggested by the gray curves in Figure 7, which show that the amplitude increases more quickly for waves with a small initial steepness as they reach their critical steepness than for waves with a high initial steepness. It is therefore more likely that they break as plunging breakers.

Waves can either break continuously – i.e. for a period of time longer than the wave period – or intermittently – i.e. the wave breaks only for a short time without losing all its energy and breaks again at a later time. The energy distribution of a breaking wave will be different for an intermittently or a continuously breaking wave. If we want to determine how a wave breaks and how much wave energy is dissipated we will have to look at a wave packet rather than a single monochromatic wave, as the wave energy is transported with the group speed.

Wave packet in an ocean an rest. First of all, let us consider a packet of wind generated deep water waves in an ocean at rest (Figure 9). At time $t = 0$, the first wave slightly exceeds the critical steepness $ka = 1/2$ and breaks (see also *Donelan* (1972)). One period later ($t = \tau$), this wave has traveled one wave length λ to the right while the shape of the wave packet has traveled $\lambda/2$ during the same time ($c_g = c/2$), i.e. the wave has traveled $\lambda/2$ relative to the packet. The steepness of this wave is therefore reduced, we assume to a value of $ka < 1/2$, and the wave does not break anymore.

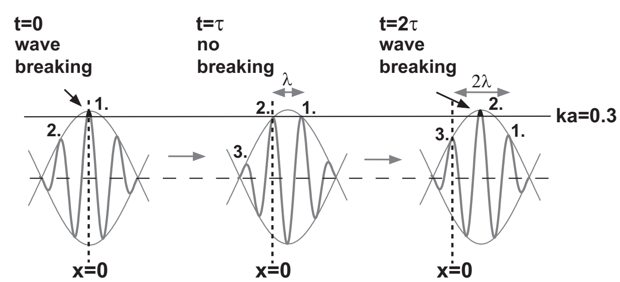

Figure 9. Intermittent breaking of a packet of deep water waves in an ocean at rest. Wave breaking occurs when the waves are steeper than the critical steepness $ka = 1/2$.

At time $t = 2\tau$, the second wave has reached its critical steepness and breaks 2τ later than the first wave and one wave length to the right of the location at which the first wave was breaking.

This intermittent breaking, however, can only occur if there is a continuous source of energy (e.g. wind) keeping the wave packet at the same amplitude. In the absence of an energy source, the steepness of the waves is reduced by wave breaking so that the waves would probably break a few times before the group decays.

Monochromatic wave on a current. With this in mind we can now look at the behavior of a quasi-monochromatic wave on a current, i.e. a wave packet that consists for any current speed u/c_0 only of one monochromatic component. Although amplitude, wave number, and wave length change due to the effect of the currents, it can be treated as a monochromatic wave, if the current speed changes only little over a wave length.

For the calculation of the energy dissipation by wave breaking, the shape of the wave packet has to be considered, as the wave energy is transported with the group speed c_g and not with the phase speed c. As already discussed (Figure 5), amplitude and wave number increase as the wave encounters an opposing current (energy given by Γ_1 in Figure 10) until it reaches its critical steepness $ka = 1/2$ (curve Υ_1) and breaks. Γ_1 and Υ_1 mark the shape of the entire wave packet at time $t = 0$.

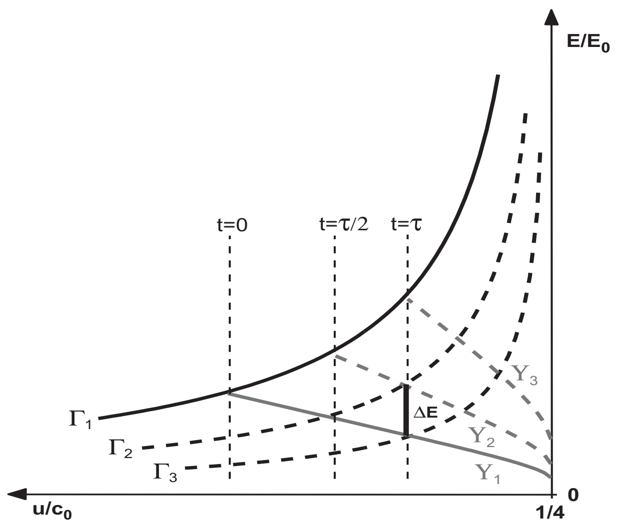

Figure 10. Behavior of a quasi-monochromatic wave on an opposing current. The normalized energy E/E_0 is given for the case without breaking (black curves Γ_i) and with breaking (gray curves Υ_j). ΔE is the energy lost by wave breaking.

As the waves travel further against the opposing current (left to the right in Figure 10), their amplitudes would increase, if they were not reduced by breaking. The energy the waves would have had without breaking is given by the curves Γ_i, with $\Gamma_i/\Gamma_1 = \text{const}$.

Let us now consider a wave that is at time $t = 0$ at location $x = 0$ (on curve Γ_1). One period τ later it has moved λ and the wave packet $\lambda/2$ to the right. If there was no wave breaking during this time, the shape of the wave packet would be given by curves Γ_1 and Υ_2. But because of breaking, the “excess” energy $\Delta E = \Upsilon_2(\lambda) - \Upsilon_1(\lambda)$ is lost between $x = 0$ and $x = \lambda$. From Figure 10 it also follows that $\Upsilon_2(\lambda) = \Gamma_2(\lambda)$. Together with

$$\frac{\Gamma_2(\lambda)}{\Gamma_1(\lambda)} = \frac{\Gamma_2(\lambda/2)}{\Gamma_1(\lambda/2)} = const. \quad \text{and} \quad \Gamma_2(\lambda/2) = \Upsilon_1(\lambda/2) \tag{11}$$

we yield an equation for the energy loss by wave breaking

$$\Delta E = \frac{\Upsilon_1(\lambda/2)\,\Gamma_1(\lambda)}{\Gamma_1(\lambda/2)} - \Upsilon_1(\lambda) \quad . \tag{12}$$

In these idealized conditions, the wave crest is continuously pushed into the region of critical steepness, so that the wave breaks continuously (and not intermittently) in order to satisfy the stability criteria. However, this is not necessarily true if the magnitude of the currents does not increase linearly or if we are looking at the more realistic case of a group of waves rather than a monochromatic wave train.

Wave packet on a current. Figure 11 shows a sketch of the break behavior of a group of waves on a current. At time $t = 0$ (a), the first wave is steeper than $ka > 1/2$ and breaks, which also changes the form of the wave packet (b). At $t = \tau$ (c), the first wave has moved $\lambda/2$ to the right (relative to the wave packet) so that its amplitude is reduced and its steepness is less than the critical value. It stops breaking. At $t = 2\tau$ (d), the next wave has reached its critical steepness and breaks – with an amplitude that is smaller than the first wave. Because the shape of the wave packet is altered by wave breaking, at a later stage (e), the waves are continuously pushed into the region of critical steepness and hence break continuously.

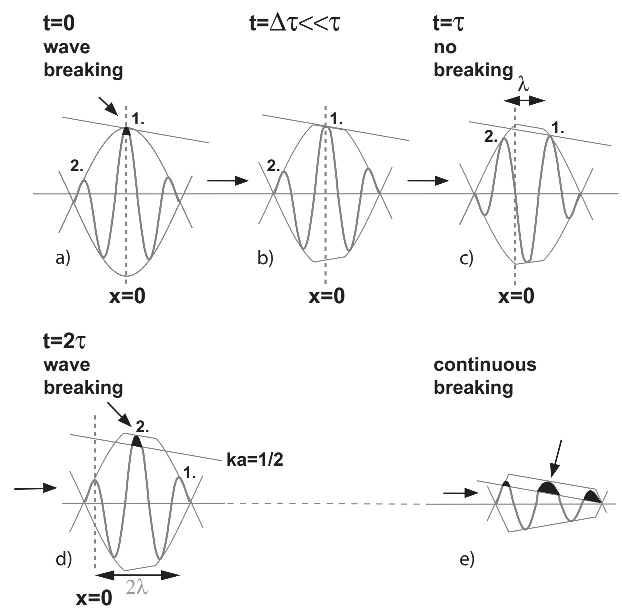

Figure 11. Sketch of the break behavior of a wave packet on a current. For explanations see text.

However, depending on the initial shape of the wave packet and the gradient in current speed, there may not be a phase of intermittent breaking. It is also possible that the waves “overshoot” when they break, i.e. the amplitude is reduced more than necessary in order to satisfy the stability criteria, and break again when they are getting too steep. The energy loss is step-like instead of continuous. Observations of breaking waves in tidal fronts (Figure 3) show, however, that most waves within the convergence zone are whitecaps, indicating that continuous breaking is predominant.

Are tidal fronts a natural laboratory to study rogue waves?

Rogue waves are a potential hazard for ships and offshore structures like oil drilling platforms. They reach wave heights of up to 35 m and exceed the significant wave height of the surrounding wave field by a factor of 1.5 - 2, so that they occur unexpectedly for ship traffic. The formation of rogue waves can be explained by the linear superposition of several waves at the same time and location due to their different phase speeds. This wave focusing can occur anywhere in the ocean but is more likely in areas of strong currents (*Wu and Yao*, 2004). However, in order to develop a forecasting and warning system it is necessary to better understand their formation mechanism and under which sea, wind, or current conditions they are likely to occur.

Observations of rogue waves, however, are very rare as they are found offshore, may be a short lived phenomenon, and occur under severe sea state conditions. The present observations have been made with wave gauges from buoys or oil drilling platforms providing time series of wave height at a fixed location (e.g. *Clauss* (2002)) and some progress has been also made with satellite measurements (*MaxWave*). These measurements, however, can only provide a snap shot in either time or space, but not both, which is necessary for observing the formation mechanism of rogue waves and their subsequent evolution.

Experiments in wave tanks offer here an advantage (e.g. *Wu and Yao*, (2004)) and have helped to understand how rogue waves can be formed. The environmental conditions, however, have to be prescribed and it can be questioned how typical they are for oceanic conditions.

It may therefore by useful to use tidal fronts as a natural laboratory as they offer advantages of both, wave tanks and natural conditions:

- tidal fronts are easily accessible; measurements from shore are possible at low cost;
- wave formation occurs even at low wind speeds and the location of tidal fronts is controlled by topography, so that this process is very predictable;
- the incoming wave field is of natural randomness;
- wave focusing due to currents favors the formation of statistically extreme waves (Figure 12).

Furthermore, because tidal fronts are on the order of 100 m wide and 1-5 km long, it is possible to carry out measurements of wave height and current speed in time and space simultaneously. For this, a land based marine radar and a (horizontally looking) moored Acoustic Doppler Current Profiler (ADCP) may be used.

It should be noted though that the environmental conditions in tidal fronts are, however, quite different from

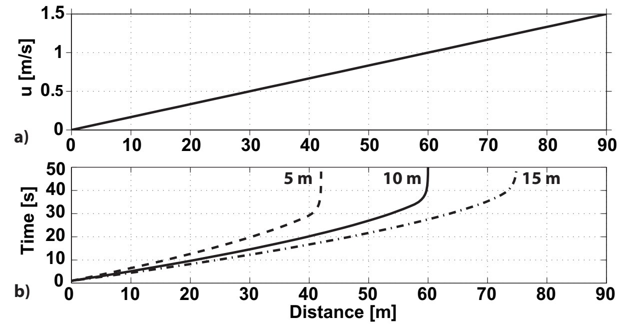

Figure 12. Wave focusing in a tidal front. As a wave encounters an opposing current it is slowed down and may be even stopped completely. For waves of different wave lengths (phase speeds) this happens at different locations within the front. The likelihood that a fast wave passes a slow wave (wave focusing) is therefore increased by the currents. a) Linearly increasing current speed ($\mathrm{m\,s^{-1}}$); b) time-space diagram of three waves with 5 m, 10 m, and 15 m wave length.

oceanic conditions under which rogue waves occur. These differences are, in particular, the one order of magnitude difference in wave height and much stronger current speed gradients that may cause wave reflection or untypical wave-wave interaction.

The principal physics of the formation process may, however, still be applicable and tidal fronts may be therefore an ideal and easily accessible natural laboratory to study the formation process of rogue waves. Other locations with similar advantages may be nearshore ocanic currents or the mouths of estuaries and rivers, where currents cause enhanced wave breaking and focusing.

Conclusions

Tidal fronts are a common and highly predictable feature of the coastal ocean. Waves that travel into the surface convergence zone of the front tend to steepen and break due to the effect of the opposing current. This process can be observed even at low wind speeds so that tidal fronts are an ideal natural laboratory for studying wave-current and wave-wave interactions.

The break behavior of waves encountering an opposing current is described by a model based on wave action conservation (*Bretherton and Garrett*, 1969). This leads to considerations of wave breaking and energy dissipation for a group of waves in the convergence zone of a tidal front. The location where a wave breaks within the tidal front is determined by its initial steepness. The break behavior of a group of waves changes from intermittend to continuous breaking as it advances against the current.

Tidal fronts may be also an ideal and easily accessible laboratory to study the formation process of statistically extreme waves as it is relatively easy to carry out simultaneous measurements in space and time. The principle physics of the formation process like wave focusing may be applicable to rogue waves in the open ocean allowing a better understanding of their formation process and hence the forecasting of these waves.

Acknowledgments. I am grateful to D.M. Farmer and C. Garrett for their inspiring supervision and many useful discussions during my PhD thesis at the University of Victoria and the Institute of Ocean Sciences, BC, Canada.

References

Baschek, B., Air-sea gas exchange in tidal fronts. PhD thesis, University of Victoria, Canada, 2003.

Bretherton, F. P., and C. J. R. Garrett, Wavetrains in inhomogeneous moving media. *Proc. Roy. Soc., 302, A*, 529-554, 1969.

Clauss, G. F., Dramas of the sea: episodic waves and their impacts on offshore structures. *Appl. Ocean Res.*, 24, 147-161, 2002.

Donelan, M., M.S. Longuet-Higgins, and J.S. Turner, Periodicity in Whitecaps. *Nature, 239*, 449-451, 1972.

Duncan, J., An experimental investigation of breaking waves produced by a towed hydrofoil. *Proc. Roy. Soc. London*, 377A, 331-348, 1980.

Farmer, D. M., R. Pawlowicz, and R. Jiang, Tilting separation flows: a mechanism for intense vertical mixing in the coastal ocean, *Dyn. Atmos. Ocean, 36*, 43–58, 2002.

Galvin, C. J., Breaker type classification on three laboratory beaches. *J. Geophys. Res., 73, 12*, 3651-3659, 1968.

Longuet-Higgins, M. S., On wave breaking and the equilibrium spectrum of wind-generated waves. *Proc. Roy. Soc., 310, A*, 151-159, 1969.

Masson, D., A case study of wave-current interaction in a strong tidal current. *J. Phys. Oceanogr*, 26(3), 359-372, 1996.

MaxWave, *http://w3g.gkss.de/projects/maxwave/*.

Phillips, O. M., *The Dynamics of the Upper Ocean*, 2nd ed., Cambridge, Cambridge University Press, 1977.

Simard, Y., D. Lavoie, and F. Saucier, Channel head dynamics: capelin (*Mallotus villosus*) aggregation in the tidally driven upwelling system of the Saguenay - St. Lawrence Marine Park's whale feeding ground, *Can. J. Fish. Aquat. Sci.*, 59(1),197-210, 2002.

Wu, C. H., and A. Yao, Laboratory measurmenets of limiting freak waves on currents. *J. Geophys. Res.*, 109, C12002, 2004.

Burkard Baschek, Woods Hole Oceanographic Institution, Marine Chemistry & Geochemistry, MS#25, Woods Hole, MA, 02543, USA. (e-mail: bbaschek@whoi.edu)

This preprint was prepared with AGU's LaTeX macros v4, with the extension package 'AGU^{++}' by P. W. Daly, version 1.6a from 1999/05/21.